Electron Ring Diagnostics With Magnetic Probes During Roll-out and Acceleration

U. Schumacher and M. Ulrich

IPP O/32 March 1976

MAX-PLANCK-INSTITUT FÜR PLASMAPHYSIK

8046 GARCHING BEI MÜNCHEN

MAX-PLANCK-INSTITUT FÜR PLASMAPHYSIK

GARCHING BEI MÜNCHEN

Electron Ring Diagnostics With Magnetic Probes During Roll-out and Acceleration

U. Schumacher and M. Ulrich

IPP O/32 March 1976

Die nachstehende Arbeit wurde im Rahmen des Vertrages zwischen dem Max-Planck-Institut für Plasmaphysik und der Europäischen Atomgemeinschaft über die Zusammenarbeit auf dem Gebiete der Plasmaphysik durchgeführt.

IPP O/32

U. Schumacher
M. Ulrich

Electron Ring Diagnostics With Magnetic Probes During Roll-out and Acceleration

Abstract

Different methods using magnetic field probes to determine the properties of electron rings during their compression, roll-out and acceleration are presented. The results of the measurements of the electron number and the axial velocity and acceleration of the rings, as obtained with the various diagnostic devices, are discussed and compared.

Zusammenfassung

Es werden verschiedene Methoden zur Bestimmung der Elektronenringeigenschaften mit Magnetfeldsonden während der Kompression, des "roll-out" und der Beschleunigung dargelegt. Die Ergebnisse der Messungen von Elektronenzahl, axialer Geschwindigkeit und Beschleunigung der Ringe, wie sie sich mit den verschiedenen Diagnostikanordnungen ergeben, werden diskutiert und miteinander verglichen.

I. Introduction

The collective acceleration of ions with relativistic electron rings[1], which allows much higher ion energy gains than in ordinary ion accelerators, uses the intense self-fields of the electron ring to couple the ions to the electrons. Owing to this strong coupling some of the ion properties (such as average axial velocity, acceleration and number ratio) can be determined from the measurements of the electron ring. By using the intense electric or magnetic fields, which surround the ring or by measuring the emitted electromagnetic radiation (Synchrotron radiation), the electron ring can be investigated during the acceleration process without destroying it.

In previous experiments, the magnetic self-field of the electron ring was used during the ring compression, mainly to determine the electron number [2]. In this report, we concentrate on the use of the ring self-field for determining the properties of the electron ring during "roll-out", i.e. transition from the compression phase to the acceleration section, and during acceleration. We are interested in the measurement of the ring velocity, acceleration, electron number, minor dimensions, and the holding power.

Other powerful ion diagnostic methods such as those using nuclear emulsions and films or nuclear reactions are not treated here because they are necessarily connected with the destruction of the ring.

II. Magnetic field measurements

a) Single-loop magnetic probes to determine N_e during compression

Magnetic probes made of a single loop have already been used to study the electron number during the electron ring compression [2]. The radial and the axial magnetic field components are proportional to the current I of the ring, but they depend on its axial

and/or radial position. The axial component B_z of a ring with a radius R, that is much larger than the loop radius R_L as well as the minor ring radius a is given on the axis and in the plane of the ring by

$$B_z = \mu_o \frac{I}{2R} \qquad \left[\text{in MKSA units}\right], \tag{1}$$

where the electron current I is related to the electron number N_e by

$$I = \frac{eN_e c}{2\pi R}, \qquad \text{so that} \tag{2}$$

$$B_z = \frac{\mu_o e c N_e}{4\pi R^2} . \tag{3}$$

The electron number evaluated from the axial magnetic field component therefore depends on the square of the radius R:

$$N_e = \frac{4\pi R^2 B_z}{\mu_o e c} \tag{4}$$

Although the effect of finite minor ring dimensions under present experimental conditions seems to be negligible [2], the R^2-dependence of N_e and the necessity of compensating the total flux of the compression magnetic field through the probe cross-section by an additional magnetic pick-up loop call for the use of the radial magnetic field component B_r of the ring to determine N_e.

Indeed, the compression magnetic field flux through the loop cross-section is very much smaller (since the magnetic field is nearly homogeneous), and one can always find a position of the loop relative to the ring such that B_r does not strongly depend on the ring radius. Magnetic probes of this type are therefore now often used. The magnitude of B_r, however, depends sensitively on the axial position of the ring relative to the probe.

The measurement of the radial or axial magnetic field component of the electron ring with single loops seems relatively easy, in so far as the ring only moves radially as during compression.

During the "roll-out" process, when the ring is transferred from the compression plane towards the acceleration section, however, the single loops lose their sensitivity, and the compensation of the outer magnetic field is very difficult, so that other types of probes must be used.

b) Probes with helical winding for determining N_e during compression and "roll-out"

If an electron ring of radius R and current I is situated at an axial distance z from a probe on the axis, its axial magnetic field component is

$$B_z = \frac{\mu_o I}{2R} \cdot \frac{1}{(1+(\frac{z}{R})^2)^{3/2}} \quad , \tag{5}$$

from which the strong axial dependence of B_z can be seen. Integrating B_z over z along the axis, however, gives a quantity that only depends on the electron current I:

$$\int_{-\infty}^{+\infty} B_z(z)\, dz = \mu_o I \quad , \tag{6}$$

which is already equal to the circumferential integral

$$\oint \vec{B}\, d\vec{s} = \mu_o I \quad ,$$

which is used in Rogowski belts.

With equ.(2) the electron number N_e is found to depend only linearly on the electron radius and is independent of the axial ring position:

(7)

The integral $\int_{-\infty}^{+\infty} B_z(z)\,dz$ does not depend on the minor axial ring dimension, and it does not change very much with the minor radial electron ring half-axis a:

$$(8) \qquad \int_{-\infty}^{+\infty} B_z(z)\,dz \approx \frac{\mu_0 e c N_e}{2\pi R}\left(1 + \frac{a^2}{3R^2}\right).$$

For $\frac{a}{R} = 0.1$ the integral increases by only $3\cdot 10^{-3}$, compared with a ring of zero minor dimensions. The integral can easily be measured with a magnetic probe of helical winding which is co-axial with the electron ring, but inside it all along the axis. The pitch of the winding should be a compromise between the sensitivity and the time resolution,(i.e.low-inductance) of the probe. The length of the probe should be chosen such that for all electron ring radii and axial positions the integral is very well approximated. If the probe extends from ζ_1 to ζ_2, with $\zeta_1 < z < \zeta_2$ and z being the ring position, the integral is

$$(9) \qquad \int_{\zeta_1}^{\zeta_2} B_z(z)\,dz = \frac{\mu_0 I}{2}\left[\frac{1}{\left(1+\left(\frac{R}{z-\zeta_1}\right)^2\right)^{1/2}} + \frac{1}{\left(1+\left(\frac{R}{\zeta_2 - z}\right)^2\right)^{1/2}}\right]$$

One already obtains more than 0.95 of the integral for $z-\zeta_1 \geq R$ and $\zeta_2 - z \geq R$. The probe length therefore should exceed the axial extent of the ring motion area (for instance, the length of the "roll-out" region) by at least three electron ring radii at each end.

Owing to its relatively high inductance the probe with the helical winding cannot be used in the electron ring acceleration-section, but it is of great advantage for determining the electron number during compression and the subsequent "roll-out" of the ring.

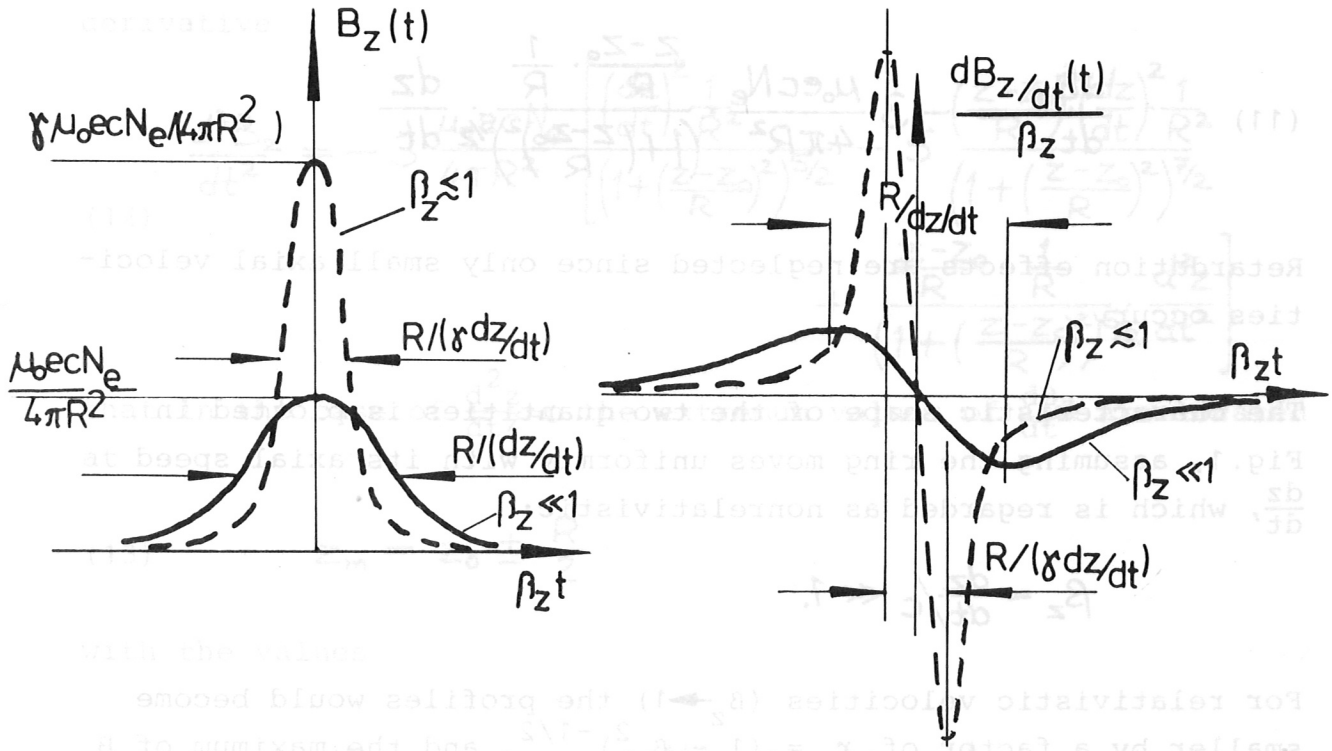

Fig.1: The axial magnetic field component and its time derivative for a uniformly moving electron ring

c) Fast single loops for the diagnostics of accelerated electron rings

As during the acceleration of the electron rings the electromagnetic fields of the ring at a certain location in laboratory space change very fast, they have to be measured with loops of very good time resolution. We concentrate here on magnetic pick-up loops on the axis that measure the axial magnetic field component B_z. The loop is located at z_o.

If the electron ring radius R and the electron number N_e are constant in time, the ring passes by, and if the minor ring dimensions are assumed to be negligible, the field $B_z(z)$ and its derivative dB_z/dt are given by:

$$B_z(z) = \frac{\mu_o ecN_e}{4\pi R^2} \cdot \frac{1}{\left(1+\left(\frac{z-z_o}{R}\right)^2\right)^{3/2}} \tag{10}$$

and

$$\frac{dB_z}{dt} = -3\,\frac{\mu_o e c N_e}{4\pi R^2}\cdot\frac{\frac{z-z_o}{R}\cdot\frac{1}{R}}{\left(1+\left(\frac{z-z_o}{R}\right)^2\right)^{5/2}}\cdot\frac{dz}{dt} \tag{11}$$

Retardation effects are neglected since only small axial velocities occur.

The characteristic shape of the two quantities is plotted in Fig.1, assuming the ring moves uniformly with its axial speed $\frac{dz}{dt}$, which is regarded as nonrelativistic:

$$\beta_z = \frac{dz}{dt}/c \ll 1.$$

For relativistic velocities ($\beta_z \to 1$) the profiles would become smaller by a factor of $\gamma = (1 - \beta_z^2)^{-1/2}$, and the maximum of B_z would increase by γ^3, too, as indicated by the dotted lines in Fig.1.

The quantity $\frac{dB_z}{dt}$ is very convenient for measurement of the ring properties since it is proportional to the voltage induced in a small loop on the axis, when the ring passes by. Under the experimental conditions it is normally not necessary to compensate the induced voltage of the main compression field.

α) Measurement of N_e

For nonrelativistic axial ring velocities the electron number N_e is determined from the maximum of $B_z(z)$ (at $z = z_o$). Its value is given by equ.(4)

ß) Determination of the axial speed $dz/dt = v_z$

There are several possibilities of measuring the axial velocity from these magnetic probe signals.

For nonuniform axial ring speed we see from equ.(11) and its derivative

$$\frac{d^2B_z}{dt^2} = -3\frac{\mu_0 e c N_e}{4\pi R^2}\left[\frac{\left(\frac{dz}{dt}\right)^2\frac{1}{R^2}}{\left(1+\left(\frac{z-z_0}{R}\right)^2\right)^{5/2}} - 5\frac{\left(\frac{z-z_0}{R}\right)^2\left(\frac{dz}{dt}\right)^2\frac{1}{R^2}}{\left(1+\left(\frac{z-z_0}{R}\right)^2\right)^{7/2}} + \frac{\frac{z-z_0}{R}\cdot\frac{1}{R}}{\left(1+\left(\frac{z-z_0}{R}\right)^2\right)^{5/2}}\cdot\frac{d^2z}{dt^2}\right] \tag{12}$$

that in the case of $\frac{d^2z}{dt^2}=0$ the extremum values of $\frac{dB_z}{dt}$ are located at

$$z_m = z_0 \pm \frac{R}{2} \tag{13}$$

with the values

$$\left.\frac{dB_z}{dt}\right|_{z_m} = -3\frac{\mu_0 e c N_e}{4\pi R^2}\cdot\frac{1}{(5/4)^{5/2}}\cdot\frac{1}{2R}\cdot\left.\frac{dz}{dt}\right|_{z_m} \tag{14}$$

which depend linearly on the ring velocity at z_m.

If $\frac{d^2z}{dt^2}$ does not vanish, but $A\cdot\frac{z_m-z_0}{R} \ll 1$ with $A = \frac{R\cdot\frac{d^2z}{dt^2}}{\left(\frac{dz}{dt}\right)^2}$, the locations of the extrema shift to

$$z_m = z_0 + \frac{A}{8}R \pm \frac{R}{2}\sqrt{1+\left(\frac{A}{4}\right)^2} \tag{15}$$

Another method of determining the axial speed $\frac{dz}{dt}$ is given by the time of flight between different magnetic probes that measure $\frac{dB_z}{dt}$ since the zero crossing of this signal accurately gives the time when the ring is at the probe location z_o. A further value is obtained from the time of flight of the ring between the two extrema, which are separated just by the amount of the electron ring radius. As can be seen from equ.(12), the slope of $\frac{dB_z}{dt}$ at z_o gives a further possibility of evaluating $\frac{dz}{dt}$.

With $$B_z(z_0) = \left| \int_{-\infty}^{t(z_0)} \frac{dB_z}{dt}\, d\tau \right| = \left| \int_{t(z_0)}^{+\infty} \frac{dB_z}{dt}\, d\tau \right|$$

the four different methods are summarized:

(16) $$\left.\frac{dz}{dt}\right|_{z_m = z_0 \pm \frac{R}{2}} = 1.16462 \cdot R \cdot \frac{\left|\frac{dB_z}{dt}(z_m)\right|}{B_z(z_0)}$$

from the extremum values of $\frac{dB_z}{dt}$,

(17) $$\overline{\frac{dz}{dt}} = \frac{R}{t_{(z_0+\frac{R}{2})} - t_{(z_0-\frac{R}{2})}}$$

from the time of flight between the extremum values of $\frac{dB_z}{dt}$,

(18) $$\left.\frac{dz}{dt}\right|_{z_0} = 0.57735 \cdot R \cdot \sqrt{\frac{\left|\frac{d^2B_z}{dt^2}(z_0)\right|}{|B_z(z_0)|}}$$

from the slope of $\frac{dB_z}{dt}$ at z_o and

(19) $$\frac{dz}{dt} = \frac{\Delta z_0}{\Delta t_{/z_0}}$$

from the time of flight of different magnetic probes.

γ) Evaluation of the electron ring acceleration $\frac{d^2z}{dt^2}$ and its holding power

The measurement of the acceleration of the electron ring is important since for unloaded rings it serves to determine the B_r in the magnetic expansion acceleration section from

(20) $$B_r\,[\text{gauss}] = 5.12141 \cdot 10^{-17}\, \frac{d^2z}{dt^2}\left[\frac{cm}{sec^2}\right]$$

if $\beta_\perp = \frac{v_\varphi}{c} \approx 1.$

Furthermore, it offers the possibility of measuring the "holding power" of the electron rings if the acceleration at a certain location in the ERA section (with a certain B_r) is measured for loaded and unloaded rings. If the acceleration increases along the acceleration section, the "holding power" of the electron rings is determined from the maximum acceleration up to which the difference in the ring inertia persists. This method has already been applied in the latest experiments [4]. The influence of the ions on the electron ring acceleration at the limit of the "holding power" (while the ions are being lost) has been numerically calculated [5].

The electron ring acceleration is evaluated as the time derivative of the axial velocity.

There is also the possibility of obtaining the acceleration from the curvature of the $\frac{dB_z}{dt}$ signal, which is normally measured. As at $z = z_o$ we have

$$\left.\frac{d^3B_z}{dt^3}\right|_{z_o} = -9\,B_z(z_o)\cdot\left.\frac{dz}{dt}\right|_{z_o}\cdot\left.\frac{d^2z}{dt^2}\right|_{z_o}\cdot\frac{1}{R^2}\,, \tag{21}$$

the electron ring acceleration can also be evaluated with equ. (18) from

$$\left.\frac{d^2z}{dt^2}\right|_{z_o} = -0.1925\,R\cdot\frac{\left.\frac{d^3B_z}{dt^3}\right|_{z_o}}{\sqrt{\left|\left.\frac{d^2B_z}{dt^2}\right|_{z_o}\right|\cdot\left|B_z(z_o)\right|}} \tag{22}$$

This value is relatively uncertain, however, since the accuracy of the amount of $\frac{d^3B_z}{dt^3}$ is small.

δ) The influence of finite minor ring dimensions on the electron ring magnetic field on the axis

Let us assume an electron ring with a rectangular density distribution of an axial extent of 2b, but negligible radial spread. The magnetic field $B_z(z)$ and its time derivative are then given

by $$B_z(z) = \frac{\mu_o e c N_e}{4\pi R^2} \cdot \frac{1}{2b} \left[\frac{z - z_o + b}{\left(1 + \left(\frac{z - z_o + b}{R}\right)^2\right)^{1/2}} - \frac{z - z_o - b}{\left(1 + \left(\frac{z - z_o - b}{R}\right)^2\right)^{1/2}} \right]$$

(24) $$\frac{dB_z(z)}{dt} = \frac{\mu_o e c N_e}{4\pi R^2} \cdot \frac{1}{2b} \left[\frac{1}{\left(1 + \left(\frac{z - z_o + b}{R}\right)^2\right)^{3/2}} - \frac{1}{\left(1 + \left(\frac{z - z_o - b}{R}\right)^2\right)^{3/2}} \right] \frac{dz}{dt} .$$

The maximum value of B_z at $z = z_o$ is changed compared with equ. (3)

(25) $$B_z(z_o) = \frac{\mu_o e c N_e}{4\pi R^2} \cdot \frac{1}{\left(1 + \left(\frac{b}{R}\right)^2\right)^{1/2}} ,$$

and the locations of the extrema of $\frac{dB_z}{dt}$ are now

(26) $$z_m \approx z_o \pm \frac{R}{2} \cdot \sqrt{1 + \frac{5}{2}\left(\frac{b}{R}\right)^2} ,$$

assuming $$\frac{d^2z}{dt^2} \ll \frac{1}{R}\left(\frac{dz}{dt}\right)^2 .$$

The different methods of determining the axial ring velocity, except the time of flight measurement with different probes, are then given by

(27) $$\left.\frac{dz}{dt}\right|_{z_m} \approx 1.1646 \, \frac{R}{B_z(z_o)} \left(1 + \frac{3}{8}\left(\frac{b}{R}\right)^2\right) \cdot \left.\frac{dB_z}{dt}\right|_{z_m}$$

from the extremum values of $\frac{dB_z}{dt}$,

(28) $$\overline{\frac{dz}{dt}} = \frac{R \cdot \sqrt{1 + \frac{5}{2}\left(\frac{b}{R}\right)^2}}{t\left(z_o + \frac{R}{2}\sqrt{1 + \frac{5}{2}\left(\frac{b}{R}\right)^2}\right) - t\left(z_o - \frac{R}{2}\sqrt{1 + \frac{5}{2}\left(\frac{b}{R}\right)^2}\right)}$$

from the ring time of flight between the two extrema of $\frac{dB_z}{dt}$ and

$$(29) \qquad \left.\frac{dz}{dt}\right|_{z_o} = 0.57735 \cdot R \cdot \sqrt{\frac{-\left.\frac{d^2B_z}{dt^2}\right|_{z_o}}{B_z(z_o)}} \left(1+\left(\frac{b}{R}\right)^2\right)$$

from the slope of $\frac{dB_z}{dt}$ at $z = z_o$.

With this last equation the acceleration of the ring can be found from the curvature of $\frac{dB_z}{dt}$ by

$$(30) \qquad \left.\frac{d^2z}{dt^2}\right|_{z_o} = -\,0.1925 \cdot R \cdot \sqrt{\frac{B_z(z_o)}{-\left.\frac{d^2B_z}{dt^2}\right|_{z_o}}} \cdot \left.\frac{d^3B_z}{dt^3}\right|_{z_o} \cdot \left(1+\left(\frac{b}{R}\right)^2\right).$$

The dependence of the magnetic field B_z (for the electron ring at z_o), that of the extremum value dB_z/dt and that of d^2B_z/dt^2 at z_o on the ratio b/R of the ring axial half-axis b to its major radius R are plotted in Figs.2 to 4, respectively. The values, normalized to those for b = 0, are partially obtained from numerical calculations and are compared with the analytic expressions. In Fig.5 the location z_m of the extremum values of $\frac{dB_z}{dt}$ is given as a function of b/R, too. The analytic solution given by equ.(26) is a very good approximation for axial extents $b/R < 0.5$.

For an electron ring of finite radial extent 2a (the electron density being inversely proportional to the radius R), the dependence of $B_z(z_o)$ and the extremum of its derivative $\frac{dB_z}{dt}$ are plotted in Figs.6 and 7. The a/R dependence of B_z is in very good agreement with the analytic result of

$$(31) \qquad B_z(z_o) = \frac{\mu_o e c N_e}{4\pi R^2} \cdot \frac{1}{2\frac{a}{R}} \ln \frac{1+\frac{a}{R}}{1-\frac{a}{R}} \; .$$

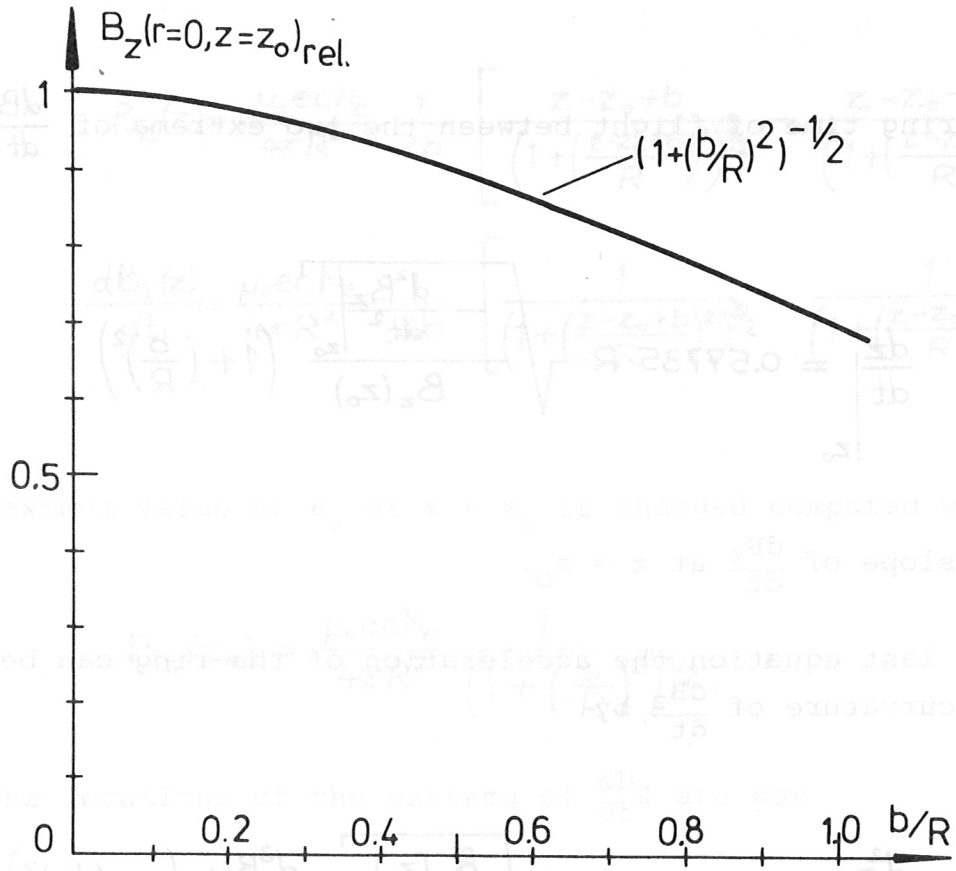

Fig.2: The axial magnetic field component B_z (relative) versus the relative axial ring half-axis b/R

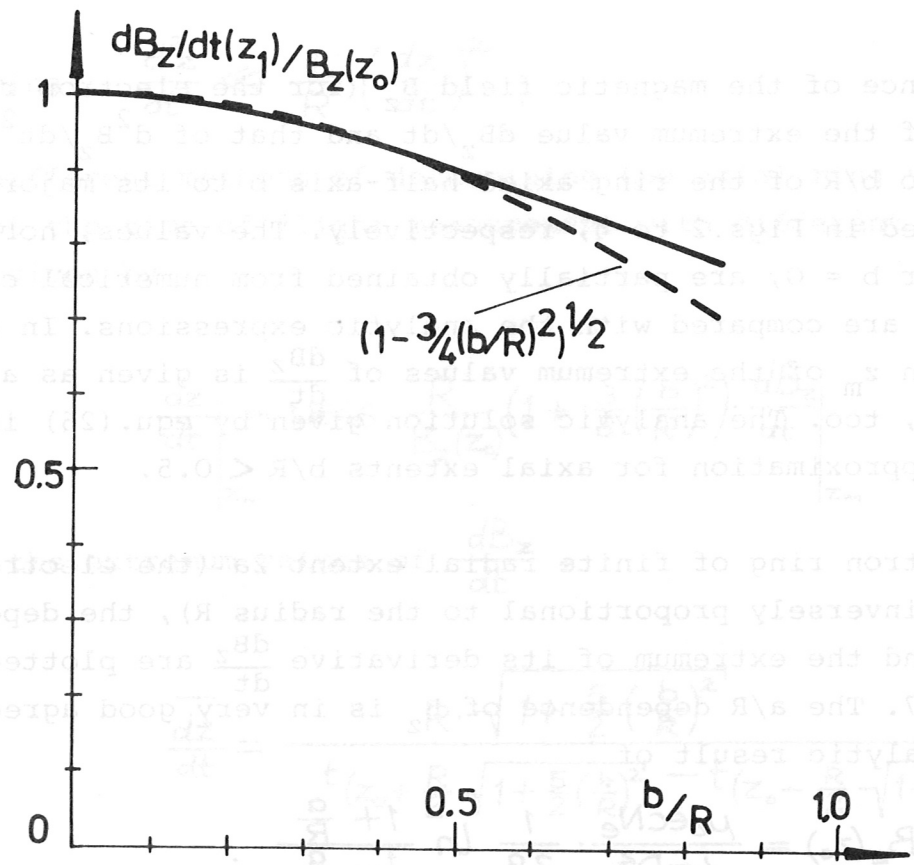

Fig.3: The time derivative $\frac{dB_z}{dt}$ (relative) versus b/R

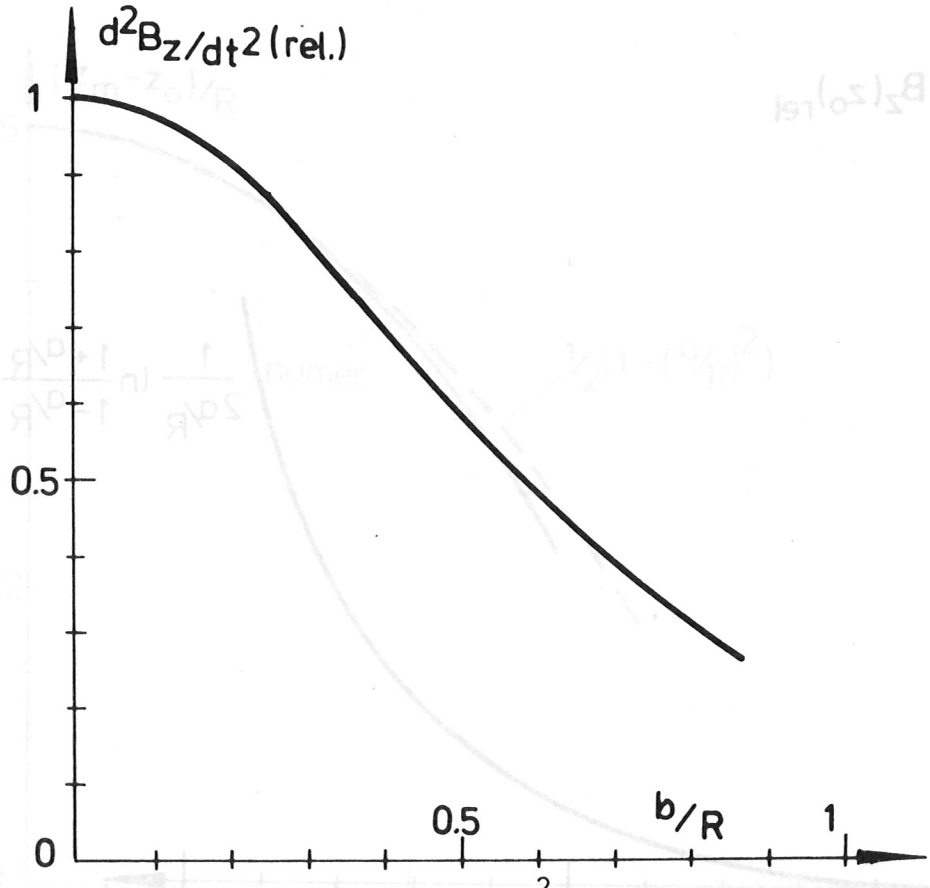

Fig.4: The relative values of $\frac{d^2B_z}{dt^2}$ versus b/R

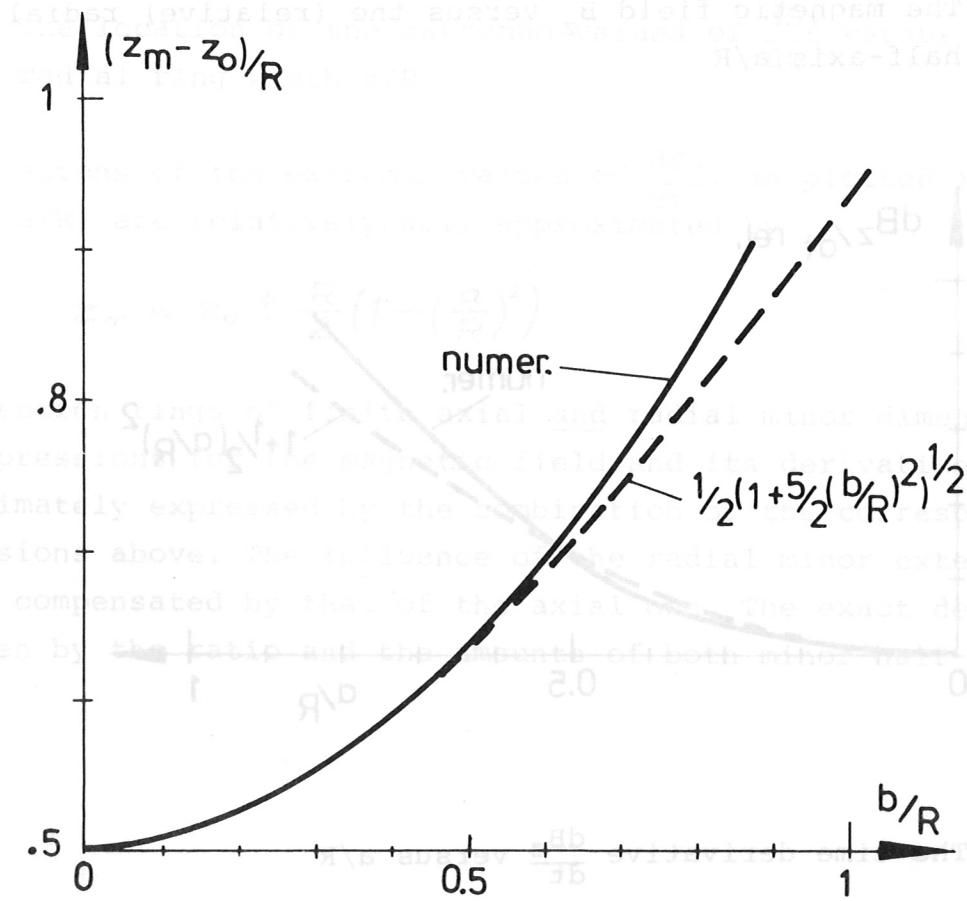

Fig.5: The location of the extremum values of $\frac{dB_z}{dt}$ versus the axial ring width b/R

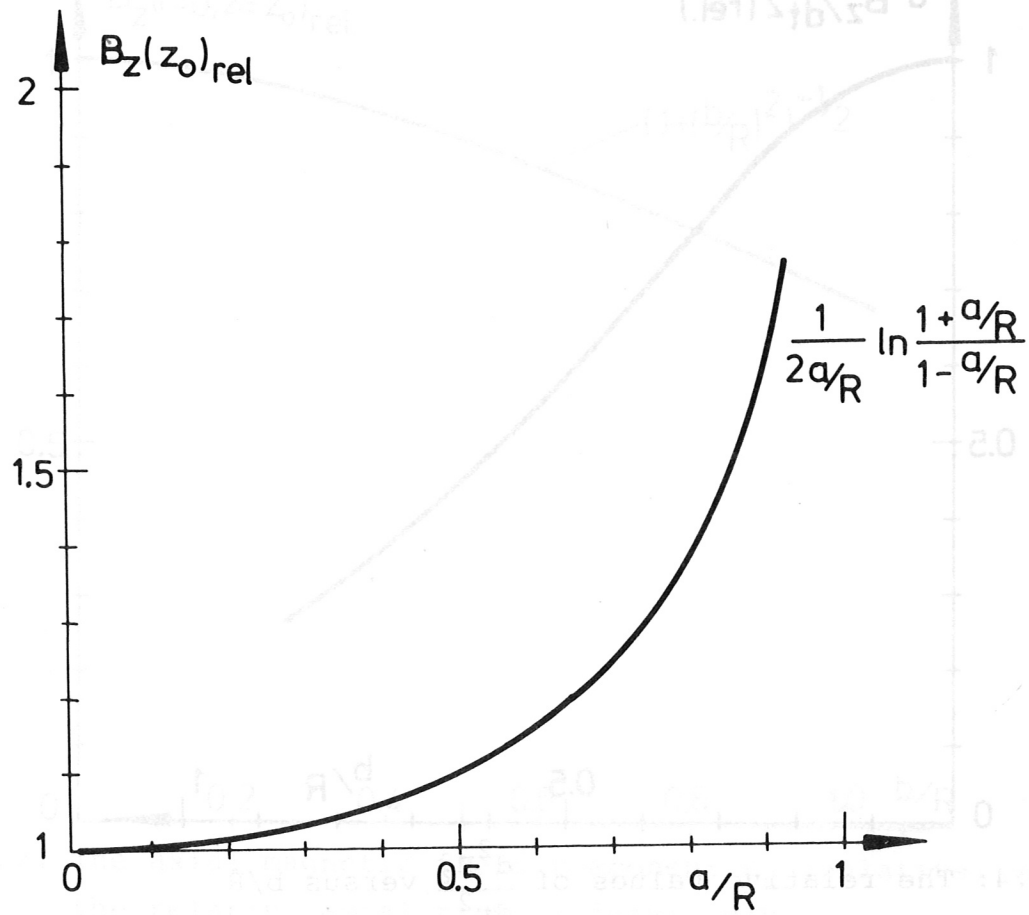

Fig.6: The magnetic field B_z versus the (relative) radial ring half-axis a/R

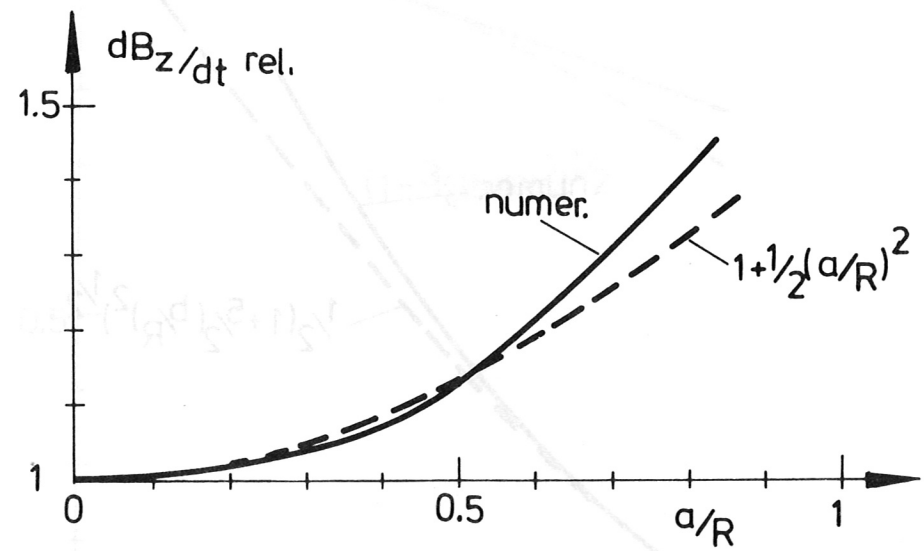

Fig.7: The time derivative $\frac{dB_z}{dt}$ versus a/R

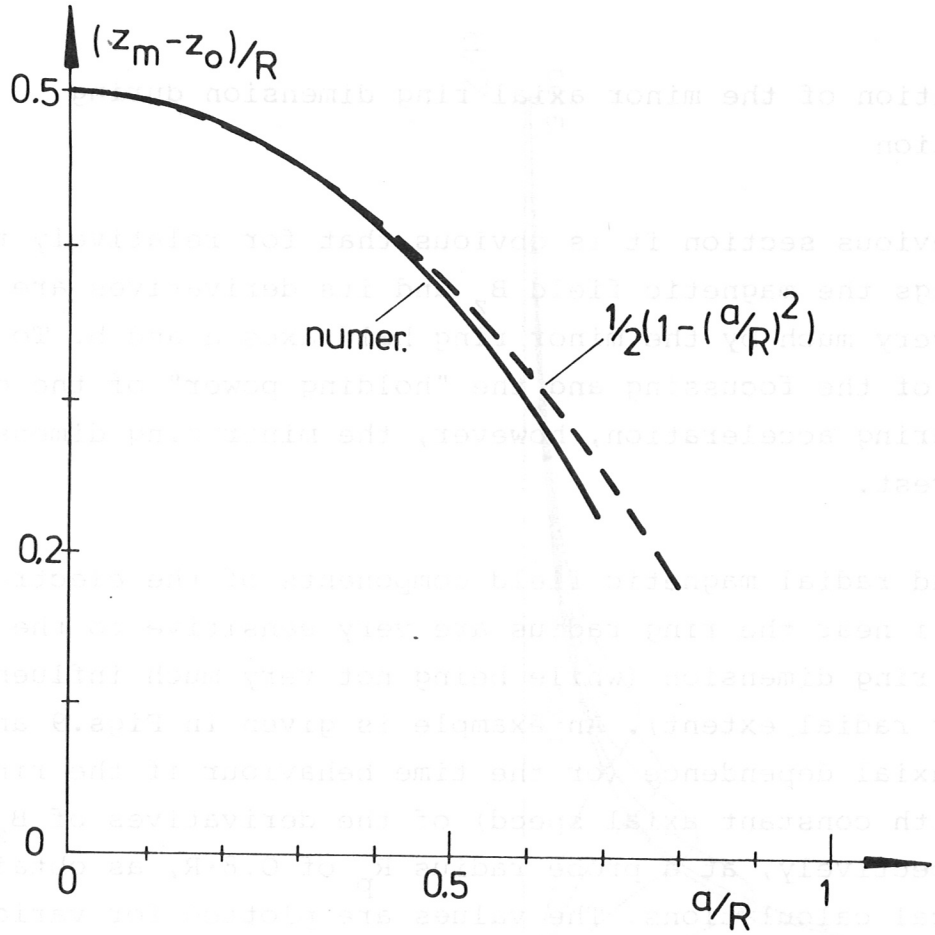

Fig.8: The location of the extremum values of $\frac{dB_z}{dt}$ versus the radial ring width a/R

The locations of the extremum values of $\frac{dB_z}{dt}$, as plotted in Fig.8 versus a/R, are relatively well approximated by

$$z_m = z_o \pm \frac{R}{2}\left(1-\left(\frac{a}{R}\right)^2\right) \tag{32}$$

For electron rings of finite axial and radial minor dimensions the expressions for the magnetic field and its derivatives can be approximately expressed by the combination of the corresponding expressions above. The influence of the radial minor extent is partly compensated by that of the axial one. The exact dependence is given by the ratio and the amounts of both minor half-axis.

ε) Determination of the minor axial ring dimension during acceleration

From the previous section it is obvious that for relatively thin electron rings the magnetic field B_z and its derivatives are not influenced very much by the minor ring half-axes a and b. To get an estimate of the focussing and the "holding power" of the electron ring during acceleration, however, the minor ring dimensions are of interest.

The axial and radial magnetic field components of the electron ring at radii near the ring radius are very sensitive to the minor axial ring dimension (while being not very much influenced by the minor radial extent). An example is given in Figs.9 and 10 for the axial dependence (or the time behaviour if the ring passes by with constant axial speed) of the derivatives of B_z and B_r, respectively, at a probe radius R_p of $0.8 \cdot R$, as obtained from numerical calculations. The values are plotted for various minor axial half-axis b, normalized to the electron radius R. It can easily be seen that the axial dependence of $\frac{dB_z}{dz}$ (and correspondingly that of $\frac{dB_z}{dt}$ for a moving ring) and, even more, that of $\frac{dB_r}{dz}$ are strongly influenced by the axial electron ring extent b/R.

The actual shape of these curves, however, will depend on the actual axial electron density distribution, so that the measurement of the time derivatives of B_r and B_z as a function of time at a fixed probe location (from which the axial distributions of the derivatives with respect to z are obtained) can only give a rough estimate for the axial ring extent.

d) Fast loop using the azimuthal magnetic field for measuring the electron ring acceleration

The evaluation of the electron ring acceleration for the local values of the ring axial velocities by differentiation calls for good reproducibility of the rings and gives results with relatively high errors. A diagnostic method directly yielding the electron

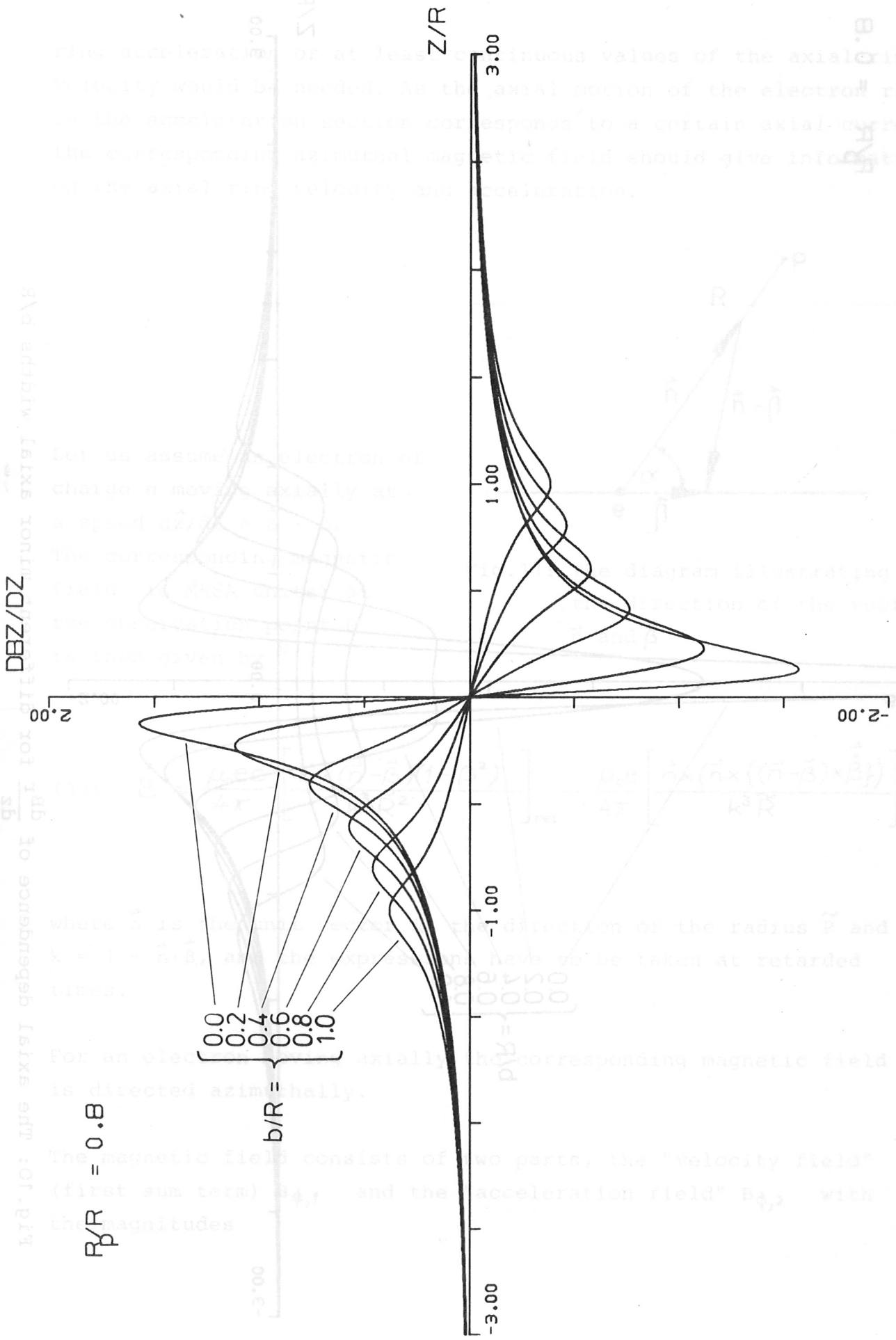

Fig.9: The axial dependence of $\frac{dB_z}{dz}$ for different minor axial widths b/R

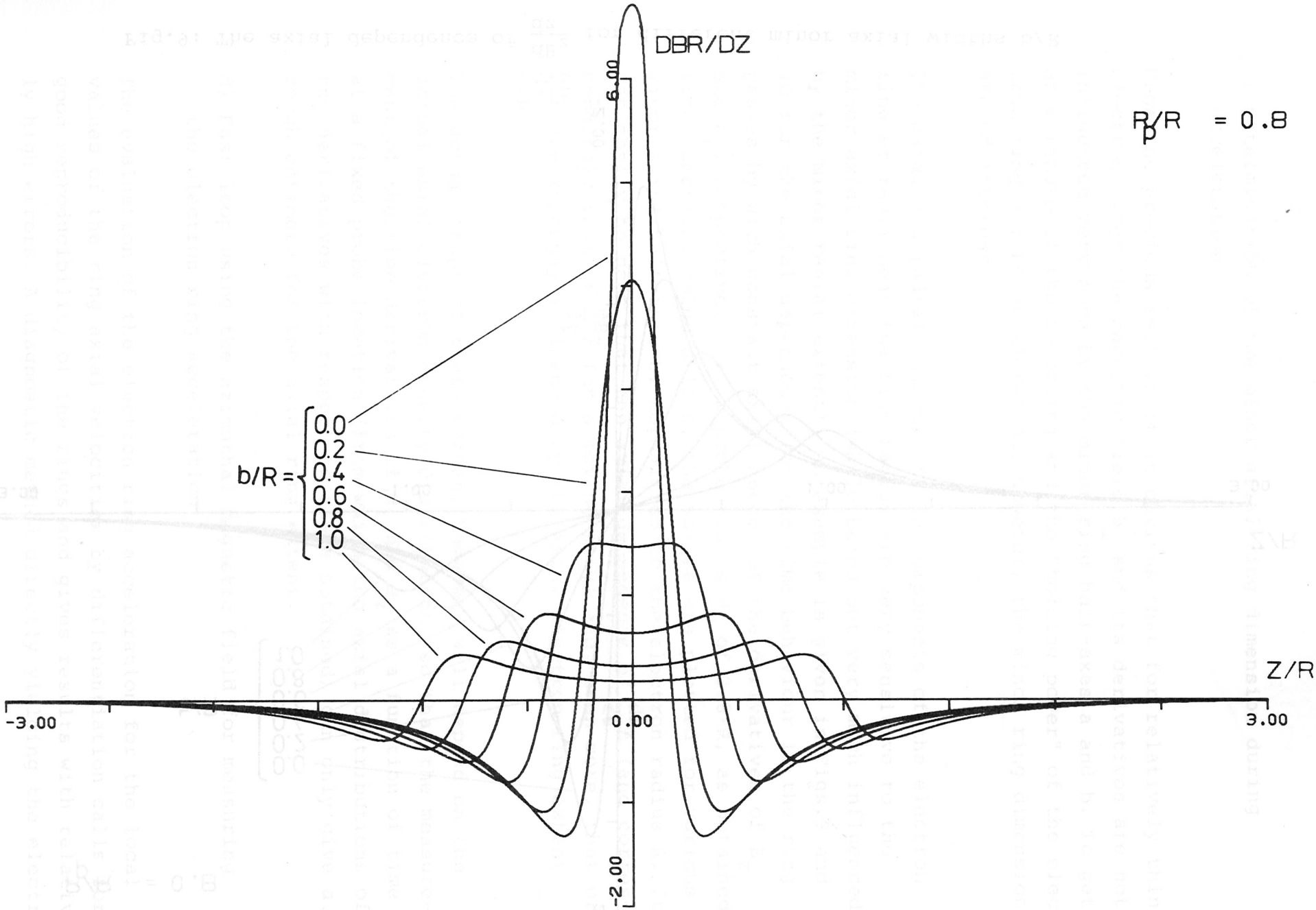

Fig.10: The axial dependence of $\frac{dB_r}{dz}$ for different minor axial widths b/R

ring acceleration or at least continuous values of the axial ring velocity would be needed. As the axial motion of the electron ring in the acceleration section corresponds to a certain axial current, the corresponding azimuthal magnetic field should give information on the axial ring velocity and acceleration.

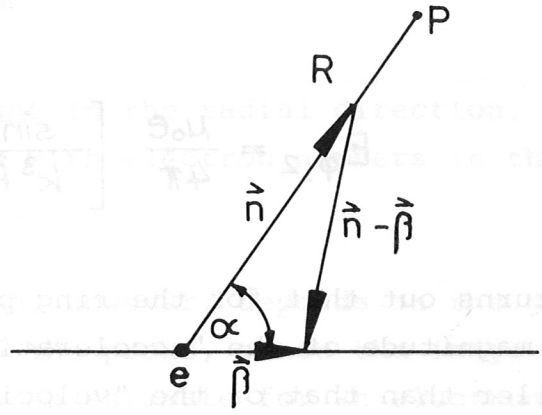

Fig.11: The diagram illustrating the direction of the vectors $\vec{n}$ and $\vec{\beta}$

Let us assume an electron of charge e moving axially at a speed $d\vec{z}/dt = \vec{\beta} \cdot c$. The corresponding magnetic field (in MKSA units) at the observation point P is then given by [6,7]

$$(33)\quad \vec{B} = \frac{\mu_0 ec}{4\pi}\left[\frac{\vec{n}\times(\vec{n}-\vec{\beta})(1-\beta^2)}{k^3\tilde{R}^2}\right]_{ret} - \frac{\mu_0 e}{4\pi}\left[\frac{\vec{n}\times(\vec{n}\times\{(\vec{n}-\vec{\beta})\times\dot{\vec{\beta}}\})}{k^3\tilde{R}}\right]_{ret}$$

where $\vec{n}$ is the unit vector in the direction of the radius $\tilde{R}$ and $k = 1 - \vec{n}\cdot\vec{\beta}$, and the expressions have to be taken at retarded times.

For an electron moving axially the corresponding magnetic field is directed azimuthally.

The magnetic field consists of two parts, the "velocity field" (first sum term) $B_{\phi,1}$ and the "acceleration field" $B_{\phi,2}$ with the magnitudes

$$(34)\qquad B_{\phi,1} = \frac{\mu_0 e c}{4\pi}\left[\frac{(1-\beta^2)\sin\alpha}{k^3\tilde{R}^2}\cdot\beta\right]_{ret}$$

and

$$(35)\qquad B_{\phi,2} = \frac{\mu_0 e}{4\pi}\left[\frac{\sin\alpha}{k^3\tilde{R}}\,\dot{\beta}\right]_{ret}$$

It turns out that for the ring parameters under investigation the magnitude of the "acceleration field" is more than two orders smaller than that of the "velocity field", so that the first one (i.e. $B_{\phi,2}$) is ignored in the following.

If we concentrate on relatively small axial velocities (i.e. $\beta \ll 1$), for which $k \approx 1$, and neglect the retardation, we get for an axially extended probe at the distance R_s from the (linear) trajectory of the electron

$$(36)\qquad \int_{-\infty}^{+\infty} B_\phi\, dz = \frac{\mu_0 e c}{4\pi R_s}\cdot 2\beta$$

with the time derivative of

$$(37)\qquad \frac{d\int_{-\infty}^{+\infty} B_\phi\, dz}{dt} = \frac{\mu_0 e c}{4\pi}\,\frac{2\dot{\beta}}{R_s}$$

As the "acceleration field" term is neglected, equ.(36) is also obtained [9] from the electric field in the frame [3], where the electron ring is at rest, and its Lorentz transformation into the Laboratory system. An example might illustrate the applicability of this method:

At a probe radius of R_s = 5 cm for an electron ring with $ß \lesssim 5 \cdot 10^{-2}$ and $\dot{ß} = 1.5 \cdot 10^{6} s^{-1}$, which corresponds to a radial magnetic field component of B_r = 2.3 G in the expansion acceleration section (see equ.(20)), one already obtains

$$\frac{d \int_{-\infty}^{+\infty} B_\phi \, dz}{dt} \approx 3 \cdot 10^{-12} \; V/cm$$

per electron and per cm probe height in the radial direction, which is easy to measure for rings with electron numbers in the range of several 10^{12}.

The induced voltage in such a probe, however, depends on the geometry of the ring surroundings and the probe, since the image currents contribute to the signal. An estimate for an electron ring of R = 2.5 cm major and a = 0.5 cm minor radius and a probe of 30 cm axial length, made up of a 0.1 cm diameter wire, which is 0.5 cm inside an outer squirrel cage structure of 3.5 cm radius, shows a reduction of the induced voltage by a factor of about 2, which is due to the image currents in the probe and the squirrel cage.

The probe gives the values of the velocity (signal integrated), the acceleration and the "holding power" of the ring.

The axially elongated probe should have a good time resolution. For higher ß the retardation and the transport of the signal on the long probe have to be taken into account.

While this type of probe has not yet been experimentally tested, experience with and the results of the other probes described are given in the following section.

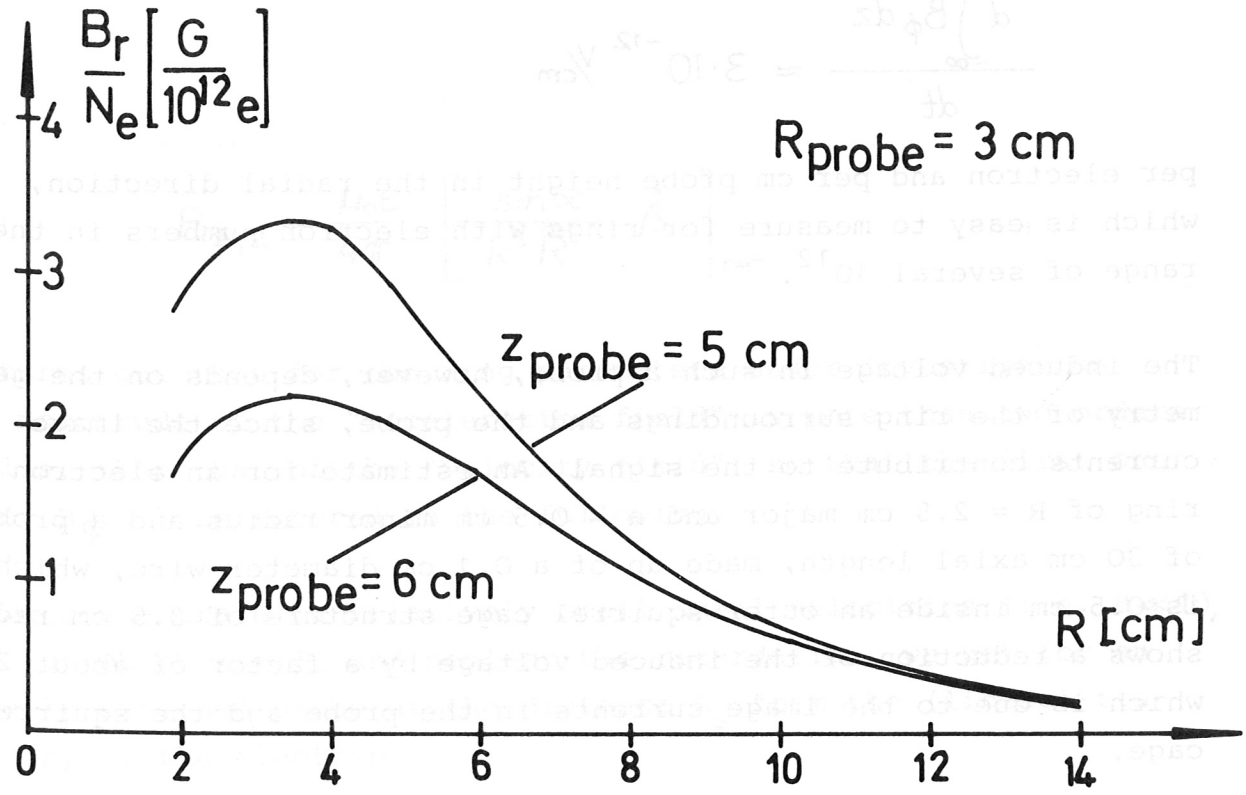

Fig.12: The sensitivity of a single loop B_r-probe versus the electron ring radius

III. The experimental arrangements and results

a) Single loop magnetic probe

During the electron ring compression in most of the recent experiments a single loop was used that measures the radial magnetic field component B_r of the ring, from which the electron number N_e in the ring is obtained. The surface of the probe lies on a cylinder of R_{probe} = 3 cm radius, while its center is located z_{probe} = 5 cm from the compression plane. Its axial extent is about 1 cm. In the azimuthal direction the probe is nearly 3 cm wide. The sensitivity of this magnetic field probe, given in Gauss per 10^{12} electrons in the ring is plotted in Fig.12 over the electron ring radius. The image currents in the surrounding compression coil [8] are taken into account. The compensation of the main compression field is performed by an additional probe outside the main coil that measures the coil return flux. The relation of the electron number N_e to the ring current I, expressed in terms of the probe sensitivity, is simply given by

$$\frac{B_r}{N_e}\left[\frac{\text{gauss}}{10^{12}\,\text{electrons}}\right] = \frac{765}{R\,[\text{cm}]} \cdot \frac{B_r}{I}\left[\frac{\text{gauss}}{\text{A}}\right] \tag{38}$$

This probe, however, is relatively sensitive to the distance z_{probe} from the compression plane, as can be seen from the curves for z_{probe} = 5 cm and z_{probe} = 6 cm in Fig.12.

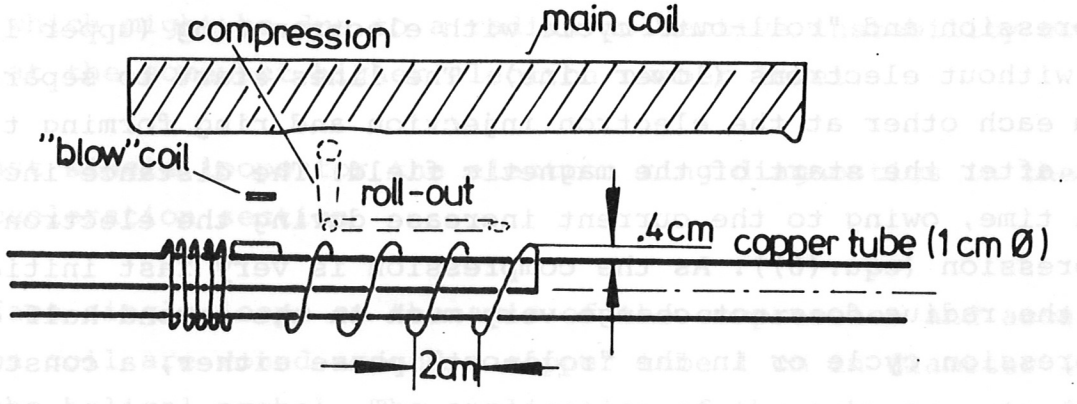

Fig.13: Schematic of the location of the probe with helical winding

b) Magnetic field probe with helical winding

A magnetic field probe with a helical winding on the compressor axis allows a measurement of the particle number in the electron rings which does not depend on the axial position of the ring, and which is only linearly dependent on the ring radius. Moreover, in a more or less homogeneous magnetic compression field, as in the present Garching electron ring experiment [4,8], there is the possibility of compensating the compression field with the same probe by the part of the helical winding with the opposite orientation, which can be seen in the schematic of Fig.13. The probe is helically wound around a copper tube 1 cm in diameter that serves as the outer conductor of a 50 Ω signal cable. The main magnetic field (and that of the ring) does not penetrate the copper tube, so that the probe area is determined by the distance (of 0.4 cm) between the winding and the tube, and inhomogeneities of the field due to the return conductor are avoided. For the whole compression and "roll-out" regions the induction probe, which measures the electron ring current, has a constant pitch of 2 cm. The compensation part (left) has the same number of windings of opposite orientation, but a smaller pitch. The axial location is chosen such that not only the compression field is compensated, but also that of the "blow" coil, which shifts the electron ring in its "roll-out" process from the compression plane to the acceleration section.

Fig.14 gives two examples of signals obtained from this probe with helical windings. Each oscillogram contains the signals from a compression and "roll-out" cycle with electron ring (upper line) and without electrons (lower line). The lines start to separate from each other at the electron injection and ring forming time just after the start of the magnetic field. The distance increases with time, owing to the current increase during the electron ring compression (equ.(6)). As the compression is very fast initially and the radius does not change very much in the second half of the compression cycle or in the "roll-out" phase either, a constant

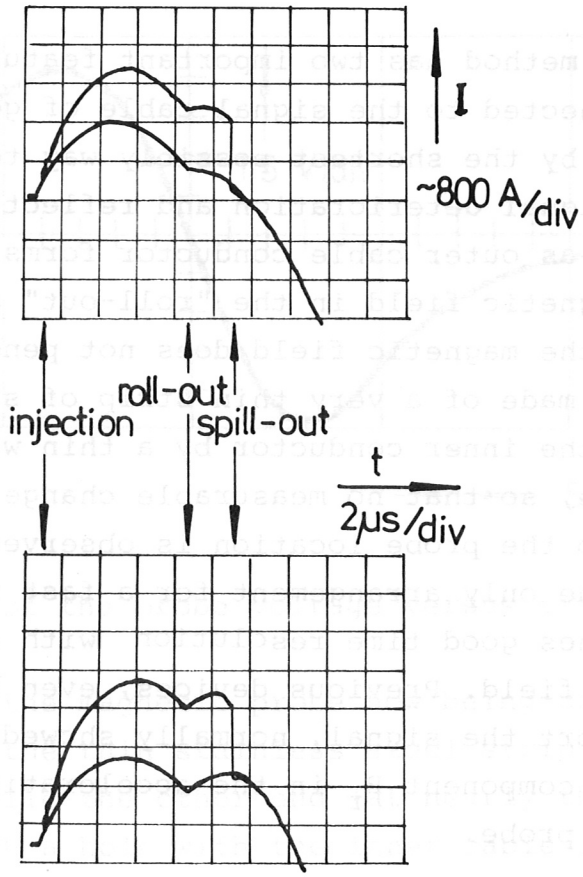

Fig.14: Two examples of signals from the probe with helical winding

separation of the signal lines means constant electron number in the ring. The upper oscillogram indicates that the electron number during the compression and the "roll-out" processes remains nearly constant up to the spill-out time, where the difference between the signal lines disappears abruptly as the ring is accelerated axially (away from the probe). The lower oscillogram, however, shows particle losses starting about 1 μs before spill-out, which might be due to a radial collective instability occuring at the somewhat higher electron number level.

c) Fast single loops for the electron ring diagnostics in the acceleration section

The fast single loops on the axis of the compression and acceleration coil are wound around a copper tube 1 cm in diameter (as for the helical probe). The application of the tube on axis for

this diagnostic method has two important features: The loop can be directly connected to the signal cable of good quality and constant impedance by the shortest possibly way to the oscilloscope, thus avoiding signal deterioration and reflections. Furthermore, the copper tube as outer cable conductor forms a very smooth boundary for the magnetic field in the "roll-out" and acceleration sections since the magnetic field does not penetrate it. The induction loop is made of a very thin strip of stainless steel connected with the inner conductor by a thin wire through a tiny hole in the tube, so that no measurable change of the main magnetic field due to the probe location is observed. This device turned out to be the only arrangement for a fast magnetic probe on axis that combines good time resolution with negligible effect on the magnetic field. Previous devices, even built from thin wires to transport the signal, normally showed an influence on the radial magnetic component B_r in the acceleration section at the location of the probe.

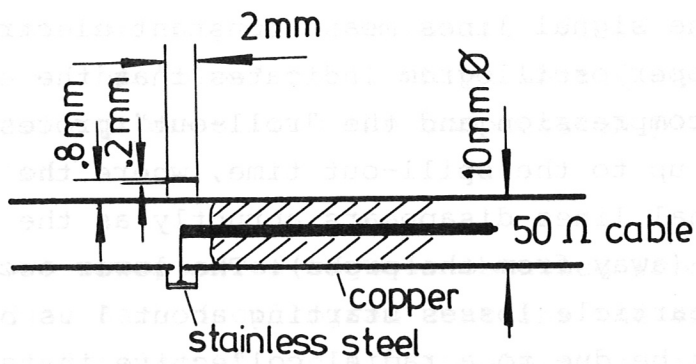

Fig.15: Cross-section of the single loop device

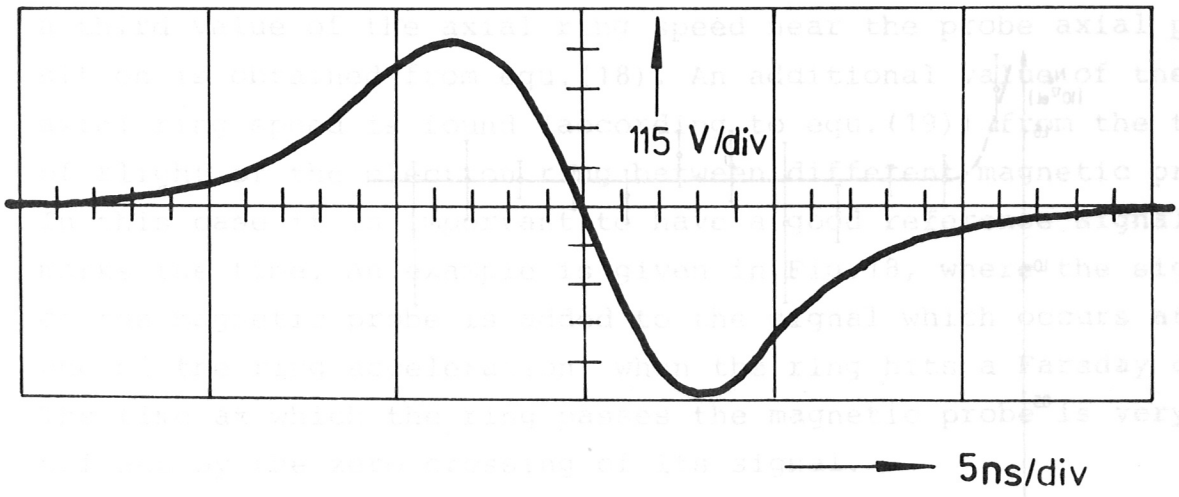

Fig.16: An example of the probe voltage versus time

A cross-section of the magnetic probe now being used is given in Fig.15. One end of the thin stainless steel strip is connected to the copper tube, while the other end (at nearly the same azimuth) is connected through a hole with the inner cable conductor. In this figure only one probe is drawn. In most cases an additional identical probe with its cable going in the opposite direction was used. The axial distance of the probes was made nearly equal to the electron ring radius in order to check the measurements according to equ.(13), especially to prove the vanishing influence of the probe on the B_r in the acceleration section. The system of probes can be brought to every desired axial location.

A typical time behaviour of the induced voltage in the probe is plotted in Fig.16, which is an oscillogram taken from TEKTRONIX 519. The voltage goes through zero at the time t_o, when the ring is at the probe location, according to equ.(11). From the dimensions of the probe (Fig.15) and equ.(3), assuming an electron ring radius of $R = 2.3$ cm, the electron number N_e is obtained from the integral $\int_{-\infty}^{t_o} U\,dt = -\int_{t_o}^{+\infty} U\,dt$ by

$$N_e = 4.06 \cdot 10^{18} \int_{-\infty}^{t_o} U\,dt\ [Vs] .$$

The signal in Fig.16 gives a result of about $N_e = 2.5 \cdot 10^{12}$.

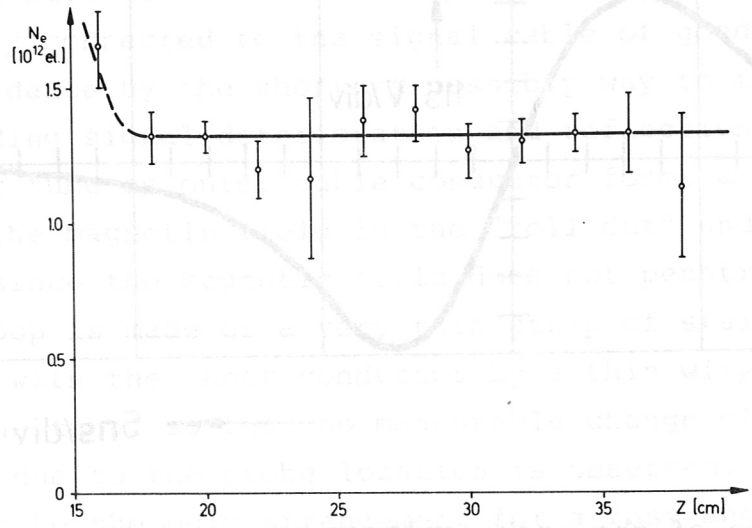

Fig.17: The axial dependence of N_e in the acceleration section

For a different set of experimental parameters the axial dependence of the electron number N_e in the ring, as obtained by this method, is plotted in Fig.17. Apart from the value just after the ring spill-out (at about z_{spill} = 15 cm), N_e seems to be constant throughout the acceleration section, which is an important condition for the interpretation of these probe signals.

As the constancy of N_e in the acceleration section can now be assumed as well as that of the electron ring radius R, further information can be obtained from the probe signals. Since in Fig.16 the extremum values are different, the electron ring velocity at axial positions of R/2 left and right of the probe location are found to be different. This means that the ring is accelerated between the two locations. The methods of determining the ring speed, described in IIc)ß), can now be applied.

From the extremum values of the measured probe voltage we get two values for the ring velocity with equ.(16). The time difference between the extremum value gives another value of the mean axial ring speed with the aid of equ.(17), while from the slope of the voltage, from which $\left|\frac{d^2B_z}{dt^2}\right|$ at the probe location is evaluated,

a third value of the axial ring speed near the probe axial position is obtained from equ.(18). An additional value of the mean axial ring speed is found (according to equ.(19)) from the time of flight of the electron ring between different magnetic probes. In this case it is important to have a good reference signal that marks the time. An example is given in Fig.18, where the signal of the magnetic probe is added to the signal which occurs at the end of the ring acceleration, when the ring hits a Faraday cup. The time at which the ring passes the magnetic probe is very well defined by the zero crossing of its signal.

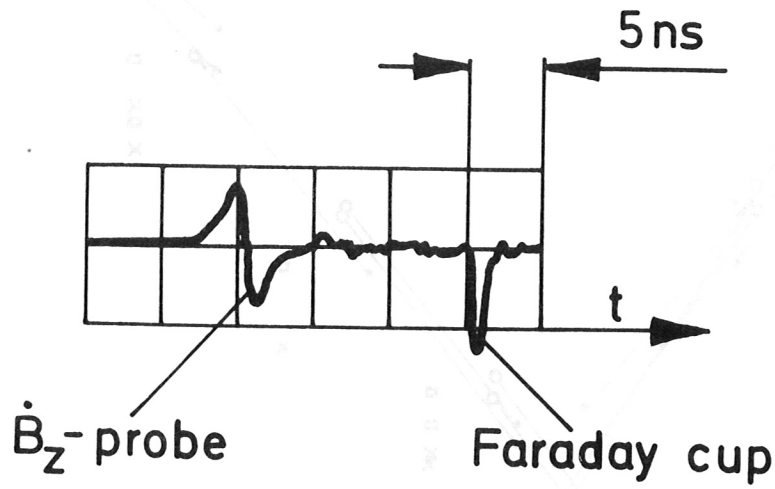

Fig.18: An oscillogram of the addition of the probe and Faraday cup signal

As an example of the different methods of determining the axial velocity v_z, Fig.19 gives the measurements of v_z as a function of the axial position z for a series of experiments with the same set of parameters, assuming the ring to have zero minor dimensions. The measurements from one shot, as obtained from the extremum values, are connected by a straight line between the abszissa z - R/2(point) and z + R/2(circle). The time of flight measurements are given by crosses, while the measurements obtained from the slope are symbolized by squares.

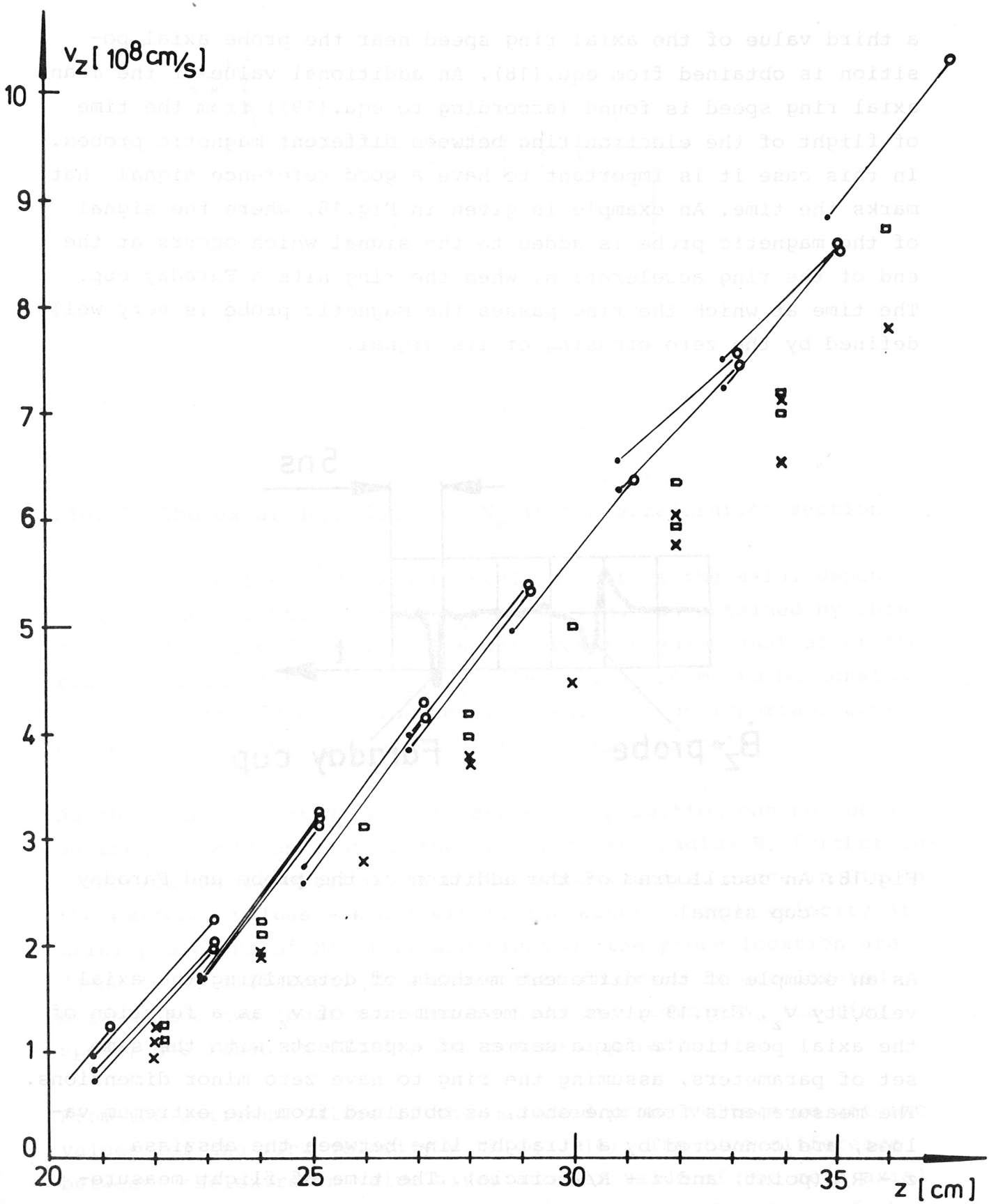

Fig.19: The axial ring velocity v_z versus z

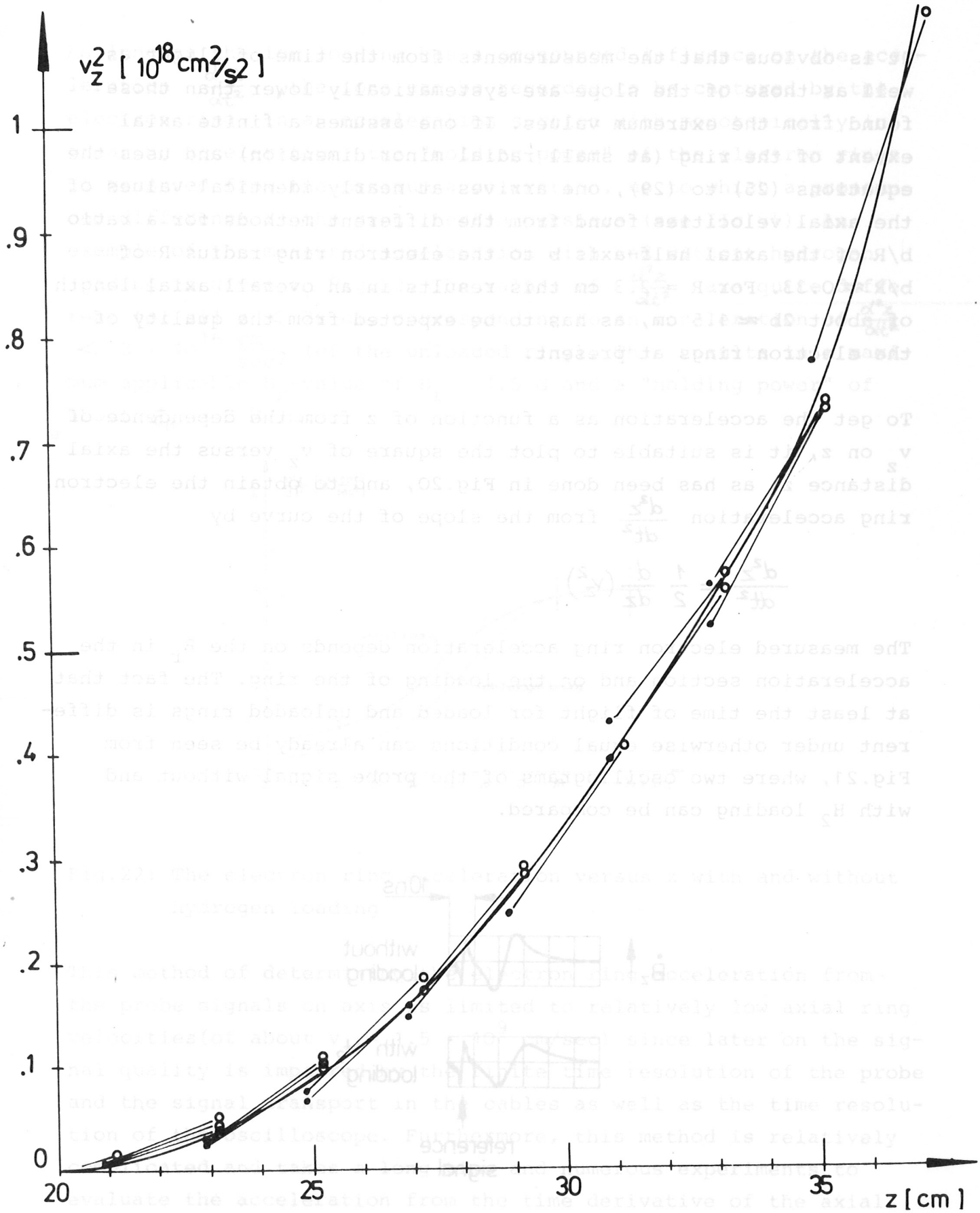

Fig.20: The square of v_z versus z

It is obvious that the measurements from the time of flight as well as those of the slope are systematically lower than those found from the extremum values. If one assumes a finite axial extent of the ring (at small radial minor dimension) and uses the equations (25) to (29), one arrives at nearly identical values of the axial velocities found from the different methods for a ratio b/R of the axial half-axis b to the electron ring radius R of $b/R \approx 0.33$. For R = 2.3 cm this results in an overall axial length of about $2b \approx 1.5$ cm, as has to be expected from the quality of the electron rings at present.

To get the acceleration as a function of z from the dependence of v_z on z, it is suitable to plot the square of v_z versus the axial distance z, as has been done in Fig.20, and to obtain the electron ring acceleration $\frac{d^2z}{dt^2}$ from the slope of the curve by

$$\frac{d^2z}{dt^2} = \frac{1}{2}\frac{d}{dz}(v_z^2)$$

The measured electron ring acceleration depends on the B_r in the acceleration section and on the loading of the ring. The fact that at least the time of flight for loaded and unloaded rings is different under otherwise equal conditions can already be seen from Fig.21, where two oscillograms of the probe signal without and with H_2 loading can be compared.

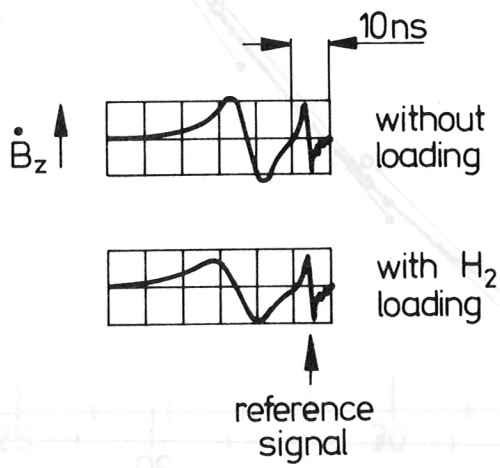

Fig.21: Comparison of magnetic probe signals with and without hydrogen loading

As long as the ion loading has a pronounced influence on the acceleration $\frac{d^2z}{dt^2}$, the ions can be regarded to be captured by the electron ring. In an acceleration section with monotonically increasing acceleration, the "holding power" of the electron rings is measured from the maximum acceleration, up to which a pronounced difference in the ring inertia persists (see IIc)γ)). An example of the measured acceleration with and without hydrogen loading is given in Fig.22. The values of $\frac{d^2z}{dt^2}$ are quite different for all $z < 26$ cm, corresponding to an acceleration of $\frac{d^2z}{dt^2} < 3 \cdot 10^{16} \frac{cm}{sec^2}$ (of the unloaded ring). This results in a maximum applicable B_r-value of $B_r = 1.5$ G and a "holding power" of about $\mathcal{E}_H = 3$ MV/m.

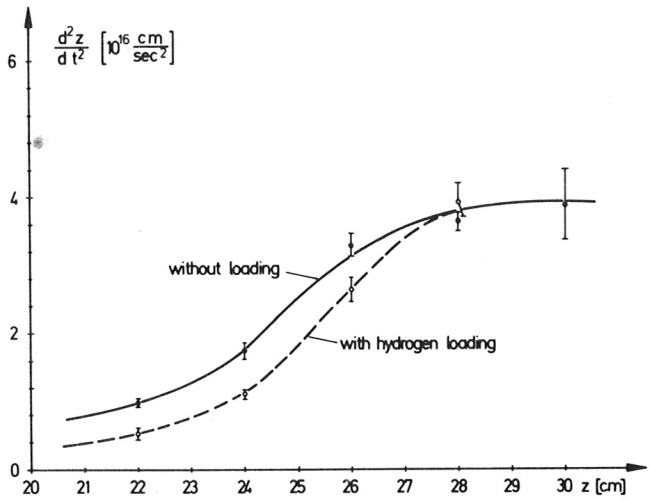

Fig.22: The electron ring acceleration versus z with and without hydrogen loading

This method of determining the electron ring acceleration from the probe signals on axis is limited to relatively low axial ring velocities(of about $v_z = 1.5 \cdot 10^9$ cm/sec) since later on the signal quality is impaired by the finite time resolution of the probe and the signal transport in the cables as well as the time resolution of the oscilloscope. Furthermore, this method is relatively complicated and takes a long time and numerous experiments to evaluate the acceleration from the time derivative of the axial velocity. It would therefore be desirable to have another diagnos-

tic method that gives the axial electron ring acceleration directly and - even more important - as a continuous function of time. This should be possible with an axially extended probe that measures the azimuthal magnetic field component of the axially accelerated ring, as described in IId). The first experiments with this method will start soon.

Acknowledgements

The authors would like to thank Dr. C. Andelfinger and Prof. A. Schlüter for comments and clarifying discussions. They are indebted to E. Springmann for carrying out the numerical calculations, as well as to P. Cierpka, G. Weber, J. Werber and A. Zacharias for carefully preparing the hardware.

References

1 V.I. Veksler et al., Proc.VI.Int.Conf.on High Energy Accelerators, 1967, Cambridge Electron Accelerator CEAL-2000, p.289 (unpublished)

2 C. Andelfinger, W. Herrmann, M. Ulrich, Max-Planck-Institut für Plasmaphysik, Garching, Report IPP 0/9 (Sept.1971)

3 J.D. Jackson, Classical Electrodynamics, p.381ff, John Wiley & Sons, Inc., New York, London, Sydney 1962

4 U. Schumacher, C. Andelfinger and M. Ulrich, Physics Letters 51 A, 367 (1975) and IEEE Trans.on Nucl.Sci.NS-22, 989 (1975)

5 U. Schumacher, Max-Planck-Institut für Plasmaphysik, Garching, Report in preparation

6 Ref.3, p.467

7 W.K.H. Panofsky and M. Phillips, Classical Electricity and Magnetism, Addison-Wesley Publ.Co., p.346, 2nd ed.,1969

8 U. Schumacher, Max-Planck-Institut für Plasmaphysik, Garching, Report IPP 0/10 (March 1972)

9 A. Schlüter, private communication